Journal of Metals, Materials and Minerals, 36(4), e2604, 2026

Sericin-mediated green production of silver nanoparticles with potent antibacterial activity against prawn pathogen *Vibrio parahaemolyticus*

Pisutsaran CHITICHOTPANYA[1,*], Chayanisa CHITICHOTPANYA[2,3], Manthana JARIYABOON[2,3], Saichalee THAPLOKA[4], Nattaya VUTHIGANOND[1], and Sarute UMMARTYOTIN[1,5,6,*]

[1] *Department of Materials and Textile Technology, Faculty of Science and Technology, Thammasat University, Pathumtani, 12120, Thailand*
[2] *Department of Chemistry, Faculty of Science, Mahidol University, Bangkok, 10400, Thailand*
[3] *Center for Surface and Engineering, Faculty of Science, Mahidol University, Nakhonpathom, 73170, Thailand*
[4] *Mae Fah Luang University Hospital, Bangkok, 10110, Thailand*
[5] *Thammasat University Center of Excellence in Smart Materials, Energy, Biochemistry, Food Technology and Textile Innovation for Sustainable Environment, Thammasat University, Patumtani, 12120 Thailand*
[6] *Center of Excellence on Petrochemical and Materials Technology, Chulalongkorn University, Bangkok, 10330, Thailand*

***Corresponding author e-mail**: pisut_c@tu.ac.th; sarute@tu.ac.th

Received date:
15 December 2025
Revised date:
12 March 2026
Accepted date:
6 July 2026

Keywords:
Silver nanoparticle;
Sericin;
Vibrio parahaemolyticus;
MIC;
MBC

Abstract

The increasing occurrence of antibiotic-resistant Vibrio species has become a major concern in aquaculture, particularly for the control of *Vibrio parahaemolyticus*, the causative agent of Acute Hepatopancreatic Necrosis Disease (AHPND), which leads to severe mortality and substantial economic losses in shrimp farming across many Asian countries. Therefore, the development of sustainable and non-antibiotic antibacterial strategies is urgently needed. In this study, silver nanoparticles (AgNPs) were synthesized using silk sericin (SS), an underutilized by-product of the sericulture industry, which served as both a natural reducing and stabilizing agent. Spherical AgNPs with a mean diameter of 12.9 ± 3.4 nm were successfully produced at an $AgNO_3$-to-SS weight ratio of 1:3 under alkaline conditions. Comprehensive physicochemical characterization confirmed their nanoscale size, high crystallinity, and strong colloidal stability for at least four weeks. Antibacterial assays showed a minimum inhibitory concentration (MIC) of 16 $\mu g \cdot mL^{-1}$ and a minimum bactericidal concentration (MBC) of 32 $\mu g \cdot mL^{-1}$ against *V. parahaemolyticus*, indicating strong antimicrobial activity of the biogenic AgNPs. These results suggest that SS-mediated AgNPs represent a promising non-antibiotic strategy for controlling *V. parahaemolyticus* infections in aquaculture. In addition, the valorization of SS into functional nanomaterials highlights its potential for broader biomedical and biotechnological applications while supporting the sustainable utilization of sericulture waste. The nanoparticles were produced through a simple, eco-friendly, low-energy one-pot synthesis that is potentially suitable for industrial-scale production.

1. Introduction

Shrimp farming is a major component of global aquaculture, generating substantial economic value and contributing significantly to domestic and international markets. This industry is particularly important in Thailand, where shrimp production plays a key role in national economic growth and export revenue [1]. However, poor management practices and increasing stocking densities have heightened the incidence of epizootic diseases, notably Acute Hepatopancreatic Necrosis Disease (AHPND), which is mainly attributed to *V. parahaemolyticus* [2]. It is a motile, rod-shaped, Gram-negative bacterium of the family Vibrionaceae and is commonly associated with aquaculture environments [3]. AHPND results in rapid and extensive damage to the shrimp hepatopancreas, a critical organ involved in digestion, nutrient absorption, metabolic regulation, and immune responses. Over the past decade, AHPND has spread across many Asian countries, causing high mortality and substantial economic losses in shrimp production [2,4]. Beyond aquaculture, *V. parahaemolyticus* is also a significant foodborne pathogen capable of inducing acute gastroenteritis in consumers and is considered one of the most critical enteric bacteria worldwide [5]. Its pathogenicity, antibiotic resistance, biofilm-forming ability, and frequent contamination in seafood have drawn increasing concern, particularly in Asia and the USA [6]. Resistance to several antibiotics such as ampicillin, rifampicin, and streptomycin has been extensively documented regarding *V. parahaemolyticus* isolated from aquatic products [7,8]. The inappropriate and excessive application of antibiotics in aquaculture has expedited the development of resistant strains, presenting significant threats to aquatic organisms and public health [9]. The rapid rise of antibiotic-resistant bacteria is now recognized as a major global health threat, underscoring the critical demand for alternative antibacterial strategies that can surpass the limits of traditional antibiotics. Among various approaches, metal nanoparticles have

emerged as promising candidates due to their potent activity against resistant pathogens [10].

Silver nanoparticles (AgNPs) are particularly recognized for their distinctive biological and physicochemical characteristics [11]. Their nanoscale size provides an elevated surface-area-to-volume proportion that improves interaction with microbial cells, ultimately disrupting cell membranes, interfering with DNA replication, and inhibiting respiration [12,13]. AgNPs demonstrate a wide range of antimicrobial efficacy upon viruses, bacteria, and fungi [14] and have shown effectiveness against Vibrio spp. in various shrimp species, including *Fenneropenaeus indicus*, *Penaeus monodon*, and *Litopenaeus vannamei* [15]. AgNPs could be produced via biological, chemical, and physical approaches [16,17]. Among these methods, chemical reduction is the most widely used, employing inorganic or organic reducing agents together with stabilizers to prevent nanoparticle aggregation. However, a major drawback of chemical synthesis is the reliance on hazardous reagents, which may pose risks to living organisms and the environment [18]. To overcome these concerns, biological or green synthesis methods have been developed. The biosynthesis of metal nanoparticles has garnered substantial interest owing to its eco-friendly nature and the utilization of biological molecules, including enzymes, microorganisms, proteins, amino acids, polyphenols, and polysaccharides, which act as natural reducing and stabilizing agents in nanoparticle formation [19]. Consequently, green-synthesized AgNPs have become particularly attractive due to their environmental compatibility and their suitability for biomedical and aquaculture applications.

Sericin (SS) is a naturally occurring macromolecular protein polymer derived from the silkworm Bombyx mori [20]. It envelops the fibroin filaments, functioning as an adhesive and protective matrix during the silk-spinning process. Traditionally, SS has been considered a waste by-product because it is eliminated and disposed of during the degumming stage of natural silk fiber production. Approximately 4,000 MT of dry silk cocoons are produced globally each year, generating around 500 MT of waste SS. Its disposal poses environmental challenges due to its high oxygen demand during degradation, which can lead to water contamination [21,22]. Valorizing SS into high-value products offers both economic and environmental benefits. Consistent with the biorefinery concept, the use of agricultural or industrial waste by-products in aquaculture and related fields is gaining attention because of their safety, environmental compatibility, and contribution to sustainable resource utilization [23]. SS exhibits notable biological activities, including antibacterial, antioxidant, and anti-inflammatory effects, while also being biocompatible and biodegradable [24]. Composed of 18 amino acids, its hydrophilic nature arises from serine-rich regions and aspartic acid residues [25]. The abundance of polar functional groups (hydroxyl, carboxyl, and amino groups) makes SS highly reactive and suitable for chemical modification. Research has also shown that hydrophilic polymers containing similar functional groups serve as reducing and stabilizing agents during the synthesis of nanoparticles [26]. Accordingly, SS has been recognized as an efficient medium for the green production of AgNPs [22,27–29]. In this system, the carboxyl groups of SS form electrostatic complexes with silver ions, while hydroxyl groups reduce Ag^{+} to metallic Ag^{0}. SS also provides a three-dimensional matrix for dense nanoparticle loading and protects AgNPs from rapid oxidation, thereby slowing the release of silver ions [28].

This study proposes an environmentally friendly and practical strategy for developing antibacterial agents targeting antibiotic-resistant *V. parahaemolyticus* for applications in shrimp aquaculture. We present a simple and efficient approach for synthesizing AgNPs using SS, which is a bio-waste from sericulture, as a natural reducing and stabilizing agent. This work focuses on the synthesis, physicochemical characterization, and antibacterial evaluation of SS-stabilized AgNPs, with the aim of transforming an underutilized waste by-product into a value-added material while addressing critical challenges in aquaculture. Comprehensive characterization of the SS-AgNPs was performed using UV–visible spectroscopy, X-ray diffraction (XRD), transmission electron microscopy (TEM), X-ray photoelectron spectroscopy (XPS), Fourier transform infrared spectroscopy (FTIR), and zeta potential analysis. Additionally, we investigated the antibacterial activity of biosynthesized AgNPs against the prawn pathogen *V. parahaemolyticus*. Our work contributes to the development of alternative antibacterial solutions that may benefit aquaculture practices and help mitigate infections impacting both humans and cultured aquatic organisms. Moreover, the valorization of SS increases the commercial potential of silk-processing by-products, thereby promoting a more sustainable sericulture industry. To our knowledge, no previous studies have particularly examined the antibacterial activity of SS–AgNPs against *V. parahaemolyticus*. This study determined the minimum inhibitory concentration (MIC) and minimum bactericidal concentration (MBC) of SS-AgNPs to assess their antibacterial efficacy. Additionally, the preparation of the SS-AgNP agent utilized in this study involves a simple, eco-friendly, and low-energy one-pot synthesis method, rendering it appropriate for potential scaling up to industrial production.

2. Materials and methods

2.1 Materials

The silk cocoons had been sourced from Kamnan-Chul Farm, Khao Kho, Thailand (Figure 1). Silver nitrate ($AgNO_3$, 99.8% purity) was procured from Carlo Erba Reagents (Bangkok, Thailand). All analytical-grade reagents utilized in this study were acquired from Sigma-Aldrich (Bangkok, Thailand).

2.2 Methods

2.2.1 Extraction of Silk Sericin

A hot water extraction technique was utilized in accordance with the procedure developed by Shaw *et al.* [22], with minor modifications. The silk cocoons were initially sliced into smaller segments. Subsequently, 10 g of these cutting cocoons were infused with 250 mL of deionized water (DI water) and 0.2% Na_2CO_3. The extraction was performed using an infrared dyeing machine (Starlet DL-6000, Daelim Starlet Co. Ltd., South Korea) for a duration of 30 min at 120°C. Subsequently, the fibroin was filtered out to obtain the SS solution through Whatman filter paper (no. 1). The SS solution was then lyophilized into a powder form using an Alpha 3-4 LSCbasic freeze-dryer (Martin Christ, Germany).

Figure 1. Images of silk cocoons.

2.2.2 Preparation of AgNPs

An aqueous $AgNO_3$ solution was prepared, employing SS as a green reducing and stabilizing agent. $AgNO_3$ and SS were mixed at varied weight ratios (1:1, 1:2, 1:3, 1:4, and 1:5) in 400 mL of DI water, with the pH subsequently adjusted to 11 using sodium hydroxide (NaOH). According to Aramwit *et al.* [27], synthesizing AgNPs in strongly alkaline conditions facilitates: (1) the complexation of amide groups from SS with silver ions, thereby preventing nanoparticle aggregation; (2) the degradation of SS under these conditions results in the formation of species that serve as reducing agents; and (3) the deprotonation of protein molecules by alkaline ions, enhancing their reducing ability toward silver ions. The reaction mixture had been stirred consistently at room temperature for 24 h to ensure complete reduction of Ag^+ ions to metallic Ag^0 nanoparticles. The resulting AgNP suspensions were characterized to determine the optimal weight ratio between $AgNO_3$ and SS utilizing a UV–visible spectrophotometer (Shimadzu UV-1800, Shimadzu Co., Japan) across a wavelength range between 325 nm and 700 nm. Zeta potential analyses were conducted utilizing a Zetasizer Nano ZS (ZEN 3600, Malvern Instruments, UK) to assess the colloidal stability and dispersion uniformity of the synthesized AgNPs.

2.2.3 Characterization of AgNPs

The particle size and morphology of the biosynthesized AgNPs were analyzed utilizing transmission electron microscopy (TEM; JEM-2100 Plus, JEOL, Japan), which was operated at a 200 kV accelerating voltage. The AgNP suspension was dispensed onto carbon-coated copper grids and permitted to air-dry under ambient conditions. A particle size distribution graph was produced by examining the dimensions of 110 AgNPs using ImageJ software. The crystalline properties of SS-AgNPs were evaluated through X-ray diffraction (XRD; D8 Discover Bruker, Germany) within the range of 25° to 80° (2θ) utilizing CuKα radiation, at 40 kV and 40 mA, with a scanning rate of $6°\cdot min^{-1}$. The particle size was determined using Scherrer's Equation [30].

$$D = \frac{k\lambda}{\beta \cos\theta} \quad (1)$$

where D represents the crystallite size (nm), and k, λ, β, and θ correspond to the Scherrer constant (0.9), X-ray wavelength (nm), full width at half maximum (FWHM), and Bragg angle, respectively.

An X-ray photoelectron spectroscopy (XPS; Kratos Axis Ultra DLD, UK) was employed for elemental analysis, and the spectra were analyzed using Vision II software. Fourier transform infrared (FTIR) spectra of SS and SS-AgNPs were obtained using a Nicolet iS50 FTIR spectrometer (Thermo Fisher Scientific, USA) over the wavenumber range of 600 cm^{-1} to 4000 cm^{-1} at a spectral resolution of 4 cm^{-1}.

2.2.4 Determination of minimum inhibitory concentration (MIC)

The MIC is the minimal concentration of an antimicrobial agent that entirely prevents the observable growth of a bacterium during a designated incubation period. The MIC of the SS-AgNPs was determined using the broth microdilution method in accordance with Clinical and Laboratory Standards Institute (CLSI, 2014) guidelines [31], with minor modifications. The *V. parahaemolyticus* strain used in this study was isolated from Vibrio-infected shrimp collected from a local shrimp farm in eastern Thailand. The strain was cultured in Tryptic Soy Broth (TSB) supplemented with 3% NaCl and incubated at 35°C for 24 h. The optical density (OD) of the bacterial suspension was adjusted to 0.08 to 0.13 at 625 nm using a spectrophotometer, corresponding to approximately 1×10^8 $CFU\cdot mL^{-1}$. The MIC assay was conducted in test tubes using a two-fold serial dilution of AgNPs. After mixing the AgNP dilutions with the standardized bacterial suspension, the final AgNP concentrations ranged from 256 $\mu g\cdot mL^{-1}$ to 2 $\mu g\cdot mL^{-1}$, with an adjusted bacterial concentration of 1×10^6 $CFU\cdot mL^{-1}$. All experiments were performed in triplicate. The inoculated tubes were incubated at 37°C for 24 h. Following incubation, bacterial growth was assessed visually by examining turbidity in each tube. The absence of turbidity indicated complete inhibition of bacterial growth. The lowest concentration of AgNPs that exhibited no visible growth was recorded as the MIC value.

2.2.5 Determination of the minimum bactericidal concentration (MBC)

The MBC is the lowest concentration of AgNPs that results in complete bacterial killing. Following MIC determination, aliquots were aseptically collected from test tubes containing AgNP concentrations ranging from the MIC value to the highest concentration tested. Each aliquot was streaked onto Tryptic Soy Agar (TSA) supplemented with 1.5% NaCl using the streak plate technique. The inoculated plates were incubated at 37°C for 24 h. After incubation, the plates were examined for visible bacterial colonies. The MBC was defined as the lowest concentration of AgNPs at which ≥99.9% of the initial bacterial population was eliminated, indicated by the absence of visible colony formation on the agar surface. A commercial antibiotic served as the positive control, whereas sterile DI water was utilized as the negative control.

2.2.6 Statistical examination

Statistical examinations were conducted utilizing SPSS software (version 20; IBM Corp., USA). Each datum is shown as mean ± standard deviation (n = 3). Group differences were evaluated through Student's t-test, with the significance level set at $p < 0.05$.

3. Results and discussion

3.1 Optimization of AgNP synthesis

The effect of the weight ratios between $AgNO_3$ and SS on AgNP formation was evaluated through UV–Vis spectroscopy. The successful synthesis of AgNPs was confirmed by a notable change in color from light yellow to yellow-brown, accompanied by a single absorption peak near 405 nm, indicative of spherical and yellow-colored AgNPs [32]. This obs ervation aligns with Mie theory, which posits that spherical nanoparticles demonstrate a singular surface plasmon resonance (SPR) band, while anisotropic particles show multiple SPR bands as a result of differing oscillation modes of conduction electrons [33]. Similar findings have demonstrated that hydrophilic polymers with hydroxyl, amino, carboxylic, phenolic, and thiol groups exhibit both reducing and stabilizing properties in nanoparticle synthesis and their overall negative charges in an alkaline environment give extra stability via electrostatic repulsion [34–36]. Among all formulations, the strongest and most well-defined absorption peak was observed at the 1:3 weight ratio ($AgNO_3$:SS), as shown in Figure 2. Therefore, this ratio was selected as the optimal ratio for the subsequent preparation and characterization of AgNP suspensions.

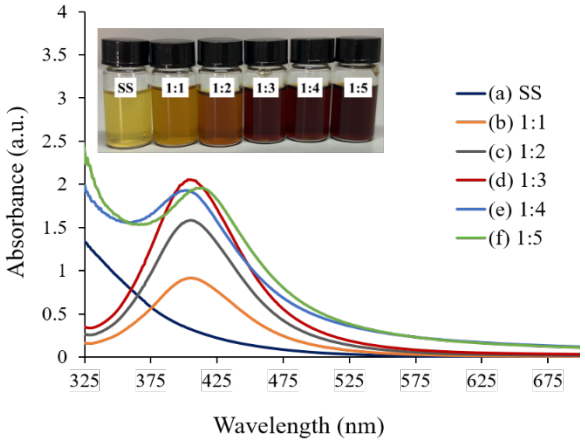

Figure 2. UV–Vis spectra of SS and AgNP suspensions at varying $AgNO_3$:SS weight ratios.

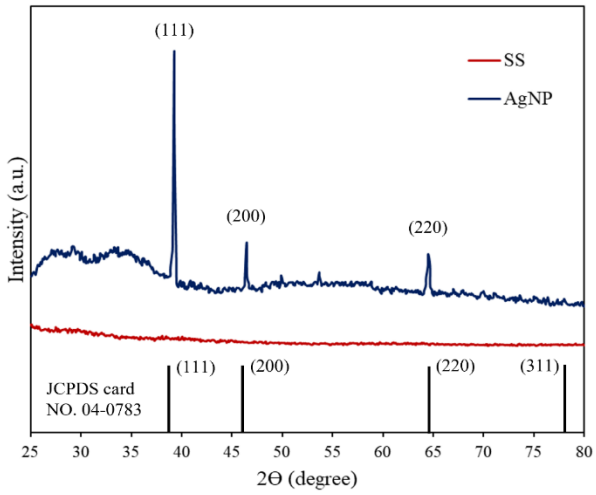

Figure 3. XRD pattern of the synthesized SS and SS-AgNPs.

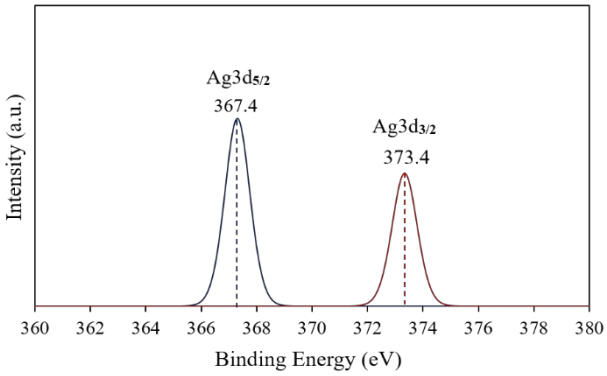

Figure 4. Deconvolution of Ag 3d of XPS spectra.

Figure 3 illustrates the XRD patterns of the optimally synthesized AgNPs, with SS serving as both the reducing and stabilizing agent. Three distinct diffraction peaks were identified for AgNPs at approximately 38.92°, 46.16°, and 64.02°, which correspond to the reflections of (111), (200), and (220), respectively. These observed characteristic peaks arise from Bragg reflections of the face-centered cubic (FCC) crystal structure of metallic Ag, thereby confirming the successful formation of crystalline AgNPs [37]. The obtained XRD pattern aligns well with previous studies [38,39] and matches the standard JCPDS file No. 04-0783. Among these, the most intense diffraction peak was observed at 38.92°, indicating that the (111) plane was the dominant crystalline orientation of the synthesized AgNPs. The average crystallite size of the AgNPs, estimated using the Debye–Scherrer equation (Equation (1)), was 12.7 nm. In contrast, pure SS exhibited no distinct diffraction peaks, indicating its amorphous nature. These results confirm the successful formation of crystalline silver nanoparticles under the optimized synthesis conditions.

Additional analysis of the oxidation state of Ag within the nanocomposites was performed using XPS. Figure 4 displays the high-solution Ag (3d) XPS spectrum. The Ag (3d) binding energy region shows two dominant peaks, with the binding energies of Ag 3d5/2 and Ag 3d3/2 at 367.4 eV and 373.4 eV, respectively, with a spin-orbit splitting of 6.0 eV, indicating a metallic state for metallic silver (Ag^0). Notably, the standard binding energies for pure silver are reported at 368.1 eV and 374.1 eV [40]. The transition of Ag 3d5/2 and Ag 3d3/2 peaks toward lower binding energies in the SS-AgNPs, relative to standard silver binding energies, may result from electron transfer between the AgNP and SS components. A similar binding energy shift has been reported by Kim *et al.* [41] for AgNPs synthesized using peptone (Pep), a soluble protein hydrolysate.

The size and morphology distribution of synthesized AgNPs were determined using TEM (Figure 5(a–b)). The AgNPs synthesized using SS exhibited a mean particle size of 12.9 ± 3.4 nm, and the corresponding particle size distribution is shown in Figure 5(c). The synthesized nanoparticles exhibited a notably spherical morphology and were well-monodispersed, and their average size was consistent with the values estimated from the XRD analysis. Overall, these characterization results confirm the successful synthesis of AgNPs using SS. Table 1 displays the zeta potential values recorded over a four-week duration, indicating the stability of the synthesized AgNPs. The SS-AgNPs exhibited a zeta potential of −34.2 ± 1.1 mV (Table 1), indicating the formation of highly stable colloidal nanoparticles. Zeta potential values that

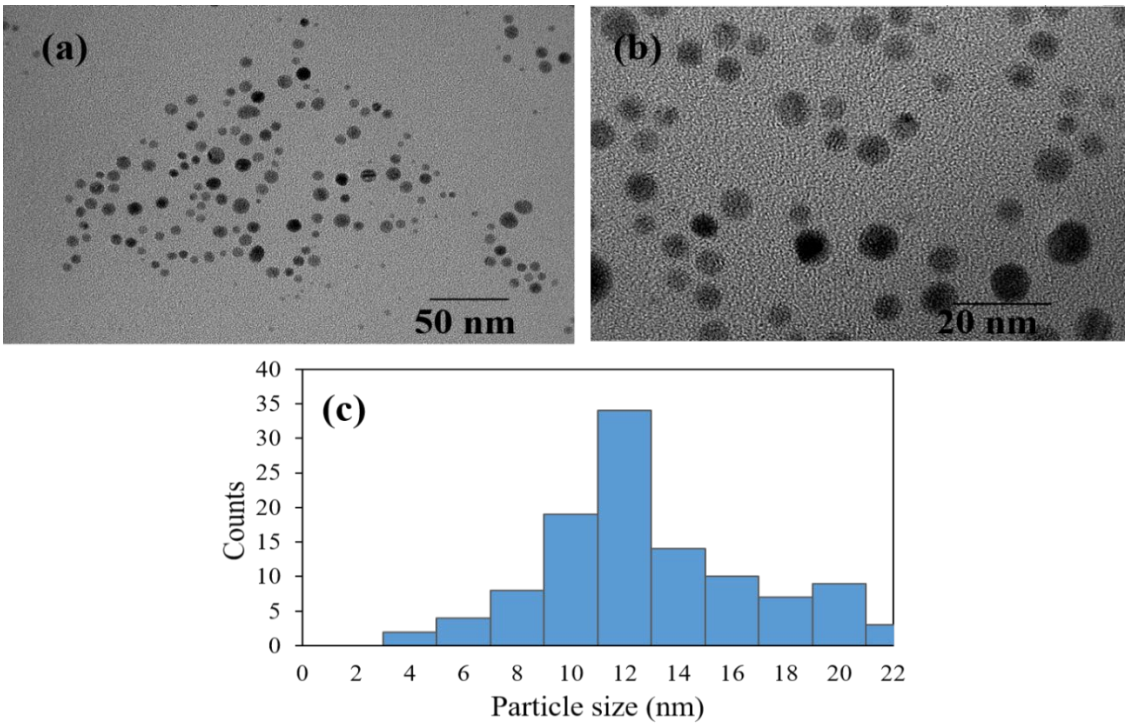

Figure 5. (a–b) TEM images of the synthesized AgNPs at magnifications of 250,000x and 300,000x, respectively; (c) particle size distribution of the AgNPs.

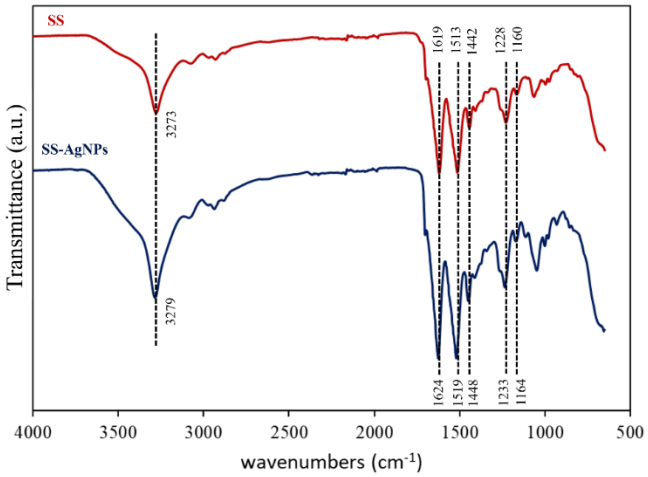

Figure 6. FTIR spectra of SS and SS-AgNPs.

Table 1. Mean zeta potentials of synthesized AgNPs for 4 weeks.

Time	Mean zeta potential [mV]
24 h	−34.2 ± 1.1
1 week	−32.8 ± 1.3
2 weeks	−31.2 ± 0.9
4 weeks	−30.2 ± 0.5

approach zero typically signify increased particle agglomeration, whereas strongly negative values enhance electrostatic repulsion, thereby improving stability and preventing aggregation [42,43]. The results in Table 1 indicate that the SS-AgNPs remained stable for at least one month, as all measured zeta potentials were consistently below −30 mV.

The FTIR spectra of SS and SS-AgNPs demonstrated the involvement of SS functional groups in the synthesis and stabilization of AgNPs. As shown in Figure 6, the broad absorption band observed at approximately 3273 cm^{-1} for SS corresponds to amide A, which is mainly associated with N–H stretching vibrations and partially overlapped with O–H stretching vibrations of hydroxyl groups. After AgNP formation, this peak shifted slightly from 3273 cm^{-1} to 3279 cm^{-1}, indicating a blue shift and suggesting interactions between the functional groups of SS and AgNPs. The FTIR spectra also exhibited three major characteristic amide bands of SS, namely amide III, amide II, and amide I, located at approximately 1228 cm^{-1}, 1513 cm^{-1}, and 1619 cm^{-1}, respectively, consistent with previous reports [29]. Following AgNP synthesis, these peaks shifted to approximately 1233 cm^{-1}, 1519 cm^{-1}, and 1624 cm^{-1}, respectively, which also represent blue shifts. These spectral changes indicate that the amide functional groups of SS participated in the reduction and stabilization of AgNPs through interactions with silver ions and nanoparticle surfaces [28]. In addition, the absence of a distinct carboxylic acid peak around 1700 cm^{-1} to 1725 cm^{-1} may be attributed to the strongly alkaline synthesis conditions. Under alkaline conditions, carboxyl groups (–COOH) of SS are likely deprotonated to carboxylate ions ($–COO^-$), resulting in the disappearance or weakening of the characteristic protonated carbonyl absorption band. Furthermore, slight peak shifts from 1142 cm^{-1} to 1148 cm^{-1} and from 1160 cm^{-1} to 1164 cm^{-1} were observed after AgNP formation, indicating changes in the chemical environment of SS functional groups and further supporting their involvement in the reduction and stabilization of AgNPs. The alkaline environment may also promote partial hydrolysis or degradation of SS molecules, exposing additional functional groups capable of donating electrons for the reduction of Ag^+ ions to metallic Ag^0 [27]. Moreover, hydroxide ions from NaOH may enhance the reducing ability of sericin by deprotonating protein functional groups, thereby increasing electron density and facilitating electron transfer during nanoparticle formation. Overall, the FTIR results confirm that sericin serves not only as a stabilizing and capping

agent but also as a reducing agent during AgNP synthesis. Functional groups including amide, hydroxyl, and carboxyl/carboxylate groups play important roles in coordinating silver ions, promoting Ag^+ reduction, and preventing nanoparticle aggregation, thereby contributing to the successful formation and stabilization of SS-AgNPs.

3.2 The MIC and MBC of Synthesized AgNPs

This study determined the MIC and MBC of synthesized AgNPs against *V. parahaemolyticus* using the broth microdilution method. The sericin-mediated green-synthesized AgNPs exhibited a MIC of 16 $\mu g \cdot mL^{-1}$ (Table 2, Figure 7) and a MBC of 32 $\mu g \cdot mL^{-1}$ (Table 3, Figure 8). These results demonstrate that the biogenic AgNPs strongly inhibited the growth of this prawn pathogen. The proposed antibacterial mechanism of AgNPs against Vibrio spp. suggests that silver ions (Ag^+) released from the nanoparticles can damage the bacterial cell wall and disrupt essential metabolic pathways, ultimately leading to protein denaturation and cell death [13]. In addition, AgNPs are known to generate high levels of reactive oxygen species (ROS) and other free radicals, which further impair cellular respiration and inhibit bacterial growth. When AgNPs are synthesized using natural bioactive extracts, the phytochemicals present in these extracts may also contribute to antibacterial and antibiofilm activity. These bioactive compounds can act synergistically with AgNPs by targeting multiple cellular pathways and metabolic processes, thereby enhancing the overall antimicrobial efficacy. The MIC and MBC values obtained in this study were lower than those reported for some other green-synthesized AgNPs against *V. parahaemolyticus*, such as those derived from *Spirulina platensis* [44] and *Camellia sinensis* [13], but higher than values reported for AgNPs synthesized using *Lysinibacillus xylanilyticus* [12]. Overall, results align with prior research indicating the significant antibacterial efficacy of AgNPs against aquaculture-associated pathogens [43,45].

The antibacterial performance of AgNPs is also strongly influenced by their physicochemical properties, particularly particle size and surface charge. In this study, the synthesized AgNPs exhibited an average diameter of 12.9 ± 3.4 nm and showed effective antibacterial activity against *V. parahaemolyticus*. Smaller nanoparticles generally exhibit enhanced antimicrobial performance due to their higher surface area-to-volume ratio, which promotes stronger interactions with bacterial cell membranes and facilitates the release of bioactive silver species [46,47]. In addition, the zeta potential reflects the surface charge and colloidal stability of nanoparticles. SS contains polar functional groups such as –OH and $–NH_2$ that can coordinate with Ag^+ ions and stabilize the formed AgNPs. Nanoparticles with higher absolute zeta potential values typically exhibit improved dispersion stability, enabling more effective contact with bacterial cells and thereby enhancing antimicrobial efficiency [48]. In the present study, the SS-AgNPs exhibited zeta potential values below −30 mV and remained stable for at least one month, indicating good colloidal stability. This stability likely helps maintain nanoparticle dispersion in suspension and contributes to the antibacterial effectiveness reflected in the observed MIC and MBC values.

However, several limitations should be acknowledged. First, the release of Ag^+ ions from SS-AgNPs was not directly quantified in this study. Instead, the antibacterial activity of the nanoparticles was evaluated. It is widely recognized that the antimicrobial activity of AgNPs arises from multiple mechanisms, including direct interaction with bacterial cell membranes, generation of ROS, and the release of Ag^+ ions into the surrounding environment [46]. Among these mechanisms, the release of Ag^+ ions is considered an important contributor to bacterial inactivation. Second, the antibacterial activity of SS alone (without AgNPs) was not experimentally evaluated. The primary objective of this work was to synthesize SS-AgNPs and investigate their antibacterial activity against *V. parahaemolyticus*. Previous studies have reported that SS itself generally exhibits weak or negligible antibacterial activity compared with AgNPs [22,28]. In this system, SS mainly functions as a reducing and stabilizing agent during nanoparticle synthesis rather than as an active antibacterial component. Therefore, the antibacterial activity observed in this study is primarily attributed to the presence of AgNPs.

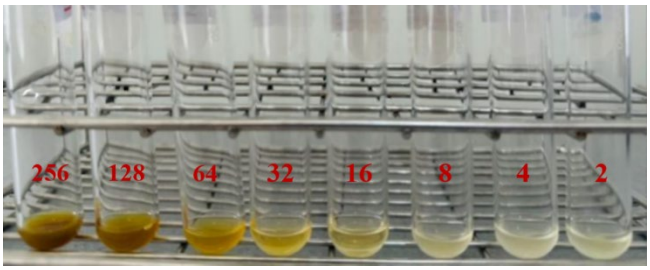

Figure 7. MIC determination of AgNPs using two-fold serial dilutions (256 $\mu g \cdot mL^{-1}$ to 2 $\mu g \cdot mL^{-1}$).

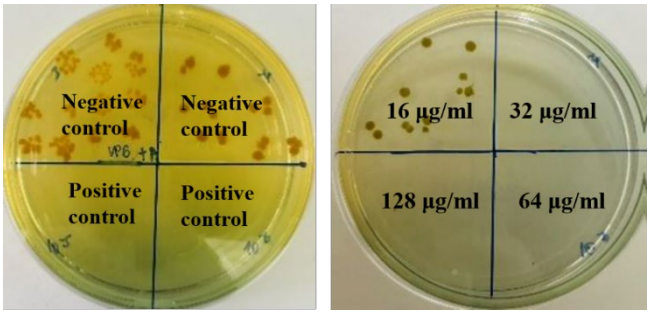

Figure 8. MBC determination of synthesized AgNPs against *V. parahaemolyticus*.

Table 2. Minimum inhibitory concentration (MIC) and turbidity of AgNPs after 24 h.

	AgNP conc. [$\mu g \cdot mL^{-1}$]							
	256	**128**	**64**	**32**	**16**	**8**	**4**	**2**
Set I	–	–	–	–	–	+	+	+
Set II	–	–	–	–	–	+	+	+
Set III	–	–	–	–	–	+	+	+

Negative (–): Absence of turbidity referring to lack of bacterial growth; Positive (+): Presence of turbidity referring to bacterial growth

Table 3. Minimum bactericidal concentration (MBC) of AgNPs after 24 h.

	AgNP conc. [μg·mL^{-1}]				Negative	Positive
	128	**64**	**32**	**16**	**control**	**control**
Set I	–	–	–	+	+	–
Set II	–	–	–	+	+	–
Set III	–	–	–	+	+	–

Negative (–): Absence of turbidity referring to lack of bacterial growth; Positive (+): Presence of turbidity referring to bacterial growth

4. Conclusion

The increasing emergence of antibiotic-resistant microbial species, particularly pathogenic Vibrio species, has become a significant concern in the aquaculture industry. In response to this issue, this work proposes an alternative approach for developing antibacterial agents targeting the antibiotic-resistant aquaculture pathogen *V. parahaemolyticus*, a major threat in shrimp farming. In this study, a green synthesis method was employed to produce AgNPs using SS, a sericulture-derived bio-waste, which serve as both a natural reducing and stabilizing agent. Spherical AgNPs with a mean diameter of 12.9 ± 3.4 nm were successfully synthesized at an $AgNO_3$-to-SS weight ratio of 1:3 under alkaline conditions. Comprehensive characterization confirmed that the SS-AgNPs possessed nanoscale dimensions, high crystallinity, and strong dispersion stability, all of which contributed to their potent antibacterial activity. The resulting nanoparticle suspension exhibited colloidal stability for at least four weeks after synthesis. Antibacterial assessment revealed MIC and MBC values of 16 μg·mL^{-1} and 32 μg·mL^{-1}, respectively, against *V. parahaemolyticus*, demonstrating the pronounced bactericidal potential of the biogenic AgNPs. Overall, the findings underscore the efficacy of SS-mediated AgNPs as a promising antimicrobial candidate for managing *V. parahaemolyticus* infections in aquaculture, offering an alternative antibacterial strategy that may enhance shrimp aquaculture health management while mitigating risks to both humans and aquatic organisms. Furthermore, this work highlights the broader applicability of SS valorization in high-value biomedical and biotechnological fields, contributing to a more sustainable and economically viable sericulture industry.

Acknowledgements

This research was supported by Thailand Science Research and Innovation (TSRI) Fundamental Fund, fiscal year 2026. This work was also supported by Thammasat University Center of Excellence in Smart Materials, Energy, Biochemistry, Food Technology and Textile Innovation for Sustainable Environment. Last, but not least, S.U. would like to acknowledge the support by Hub of Talent: Sustainable Materials for Circular Economy, National Research Council of Thailand (NRCT). We also gratefully acknowledge Dr. Saichalee Thaploka as an essential intellectual contributor to this work.

References

[1] Y. Kittichotsatsawat, W. Wattanutchariya, A. Jongjareonrak, and P. Seesuriyachan, "Enhancing manufacturing operations within the supply chain for sustainable frozen shrimp production," *Sustainability,* vol. 17, p. 2412, 2025.

[2] H. M. Santos, C.-Y. Tsai, K. R. A. Maquiling, L. L. Tayo, A. R. Mariatulqabtiah, C.-W. Lee, and K. P. Chuang, "Diagnosis and potential treatments for acute hepatopancreatic necrosis disease (AHPND): a review," *Aquaculture International*, vol. 28, no. 1, pp. 169–185, 2020.

[3] X. Zheng, J. Guo, H. Rao, D. Guo, Y. Huang, Y. Xu, S. Liang, X. Xia, and C. Shi, "Antibacterial and antibiofilm activity of coenzyme Q0 against *Vibrio parahaemolyticus*," *Food Control,* vol. 109, p. 106955, 2020.

[4] V. Kumar, S. Roy, B. K. Behera, P. Bossier, and B. K. Das, "Acute hepatopancreatic necrosis disease (AHPND): virulence, pathogenesis and mitigation strategies in shrimp aquaculture," *Toxins,* vol. 13, p. 524, 2021.

[5] M. Ashrafudoulla, M. F. R. Mizan, A. J. Ha, S. H. Park, and S. D. Ha, "Antibacterial and antibiofilm mechanism of eugenol against antibiotic resistance *Vibrio parahaemolyticus*," *Food Microbiology,* vol. 91, p. 103500, 2020.

[6] H. A. Ahmed, R. M. El Bayomi, M. A. Hussein, M. H. E. Khedr, E. M. Abo Remela, and A. M. M. El-Ashram, "Molecular characterization, antibiotic resistance pattern and biofilm formation of *Vibrio parahaemolyticus* and *V. cholerae* isolated from crustaceans and humans," *International Journal of Food Microbiology,* vol. 274, pp. 31–37, 2018.

[7] S. Elmahdi, L. V. DaSilva, and S. Parveen, "Antibiotic resistance of *Vibrio parahaemolyticus* and *Vibrio vulnificus* in various countries: a review," *Food Microbiology,* vol. 57, pp. 128–134, 2016.

[8] C. W. Tan, Y. Rukayadi, H. Hasan, T. Y. Thung, E. lee, W. D. Rollon, H. Hara, A. Y. Kayali, M. Nishibuchi, and S. Radu, "Prevalence and antibiotic resistance patterns of *Vibrio parahaemolyticus* isolated from different types of seafood in Selangor, Malaysia," *Saudi Journal of Biological Sciences,* vol. 27, no. 6, pp. 1602–1608, 2020.

[9] F. C. Cabello, "Heavy use of prophylactic antibiotics in aquaculture: a growing problem for human and animal health and for the environment," *Environmental Microbiology,* vol. 8, pp. 1137–1144, 2006.

[10] C. Prabhu, A. U. Satyaprasad, and V. K. Deekshit, "Understanding bacterial resistance to heavy metals and nanoparticles: mechanisms, implications, and challenges," *Journal of Basic Microbiology,* vol. 65, p. e2400596, 2025.

[11] M. Kandiah, and L. N. De Silva, "Microwave-assisted ecofriendly silver nanoparticle synthesis by varieties of Chrysanthemum morifolium Ramat: Assessing their antioxidant, photocatalytic

and antibacterial activities," *Journal of Metals, Materials and Minerals,* vol. 31, pp. 51–61, 2021.

[12] M. A. Huq, "Biogenic silver nanoparticles synthesized by *Lysinibacillus xylanilyticus* MAHUQ-40 to control antibiotic-resistant human pathogens *Vibrio parahaemolyticus* and *Salmonella Typhimurium*," *Frontiers in Bioengineering and Biotechnology,* vol. 8, p. 2020, 2020.

[13] S. K. I, R. Soundharajan, and H. Srinivasan, "Camellia sinensis mediated nanoparticles to control growth and biofilm in Vibrio sp.," *Aquaculture International,* vol. 33, p. 204, 2025.

[14] C. Vanlalveni, S. Lallianrawna, A. Biswas, M. Selvaraj, B. Changmai, and S. L. Rokhum, "Green synthesis of silver nanoparticles using plant extracts and their antimicrobial activities: A review of recent literature," *RSC Advances,* vol. 11, pp. 2804–2837, 2021.

[15] L. Camacho-Jiménez, A. R. Álvarez-Sánchez, and C. H. Mejía-Ruíz, "Silver nanoparticles (AgNPs) as antimicrobials in marine shrimp farming: A review," *Aquaculture Reports,* vol. 18, p. 100512, 2020.

[16] N. H. Hoang, V. N. Nguyen, T. T. Nguyen, and T. M. D. Nguyen, "Impact of microwave synthesis time on the shape of silver nanostructures and their antibacterial activity," *Journal of Metals, Materials and Minerals,* vol. 33, pp. 101–106, 2023.

[17] G. Magdy, E. Aboelkassim, S. M. Abd Elhaleem, and F. Belal, "A comprehensive review on silver nanoparticles: Synthesis approaches, characterization techniques, and recent pharmaceutical, environmental, and antimicrobial applications," *Microchemical Journal,* vol. 196, p. 109615, 2024.

[18] K. Khosravi-Katuli, E. Prato, G. Lofrano, M. Guida, G. Vale, and G. Libralato, "Effects of nanoparticles in species of aquaculture interest," *Environmental Science and Pollution Research,* vol. 24, pp. 17326–17346, 2017.

[19] T. Sutjaritvorakul, and S. Chutipaijit, "Biogenic synthesis and antibacterial activity of silver nanoparticles (AgNPs) produced by Phomopsis sp. strain GFPA2," *Biomass Journal of Metals, Materials and Minerals,* vol. 28, pp. 41–46, 2019.

[20] R. I. Kunz, R. M. C. Brancalhão, L. F. C. Ribeiro, and M. R. M. Natali, "Silkworm sericin: properties and biomedical applications," *BioMed Research International,* vol. 2016, p. 8175701, 2016.

[21] S. Seo, G. Das, H. Shin, and J. K. Patra, "Silk sericin protein materials: Characteristics and applications in food-sector industries," *International Journal of Molecular Sciences,* vol. 24, p. 4951, 2023.

[22] S. Shaw, R. Mondal, P. Dam, A. Mandal, R. Acharya, S. Manna, D. Gangopadhyay, and A. K. Mandal, "Synthesis, characterization and application of silk sericin-based silver nanocomposites for antibacterial and food coating solutions," *RSC Advances,* vol. 14, no. 45, pp. 33068–33079, 2024.

[23] S. S. Mathew, H. J. Maria, B. J. Allardyce, R. Rajkhowa, and S. Thomas, "Waste to wealth: exploring the versatile prospects of discarded silk sericin," *ACS Sustainable Chemistry & Engineering,* vol. 12, pp. 1165-1184, 2024.

[24] J. Liu, L. Shi, Y. Deng, M. Zou, B. Cai, Y. Song, Z. Wang, and L. Wang, "Silk sericin-based materials for biomedical applications," *Biomaterials,* vol. 287, p. 121638, 2022.

[25] J. Wang, H. Liu, X. Shi, S. Qin, J. Liu, Q. Lv, J. Liu, Q. Li, Z. Wang, and L. Wang, "Development and application of an advanced biomedical material-silk sericin," *Advanced Materials,* vol. 36, no. 23, p. 2311593, 2024.

[26] S. Ravindra, Y. M. Mohan, N. N. Reddy, and K. M. Raju, "Fabrication of antibacterial cotton fibres loaded with silver nanoparticles via "green approach," *Colloids and Surfaces A: Physicochemical and Engineering Aspects,* vol. 367, pp. 31–40, 2010.

[27] P. Aramwit, N. Bang, J. Ratanavarapor,n and S. Ekgasit, "Green synthesis of silk sericin-capped silver nanoparticles and their potent anti-bacterial activity," *Nanoscale Research Letters,* vol. 9, p. 79, 2014.

[28] P. Chitichotpanya, and C. Chitichotpanya, "In vitro assessment of sericin-silver functionalized silk fabrics for enhanced UV protection and antibacterial properties using experimental design," *Coatings,* vol. 7, p. 145, 2017.

[29] H. He, G. Tao, Y. Wang, R. Cai, P. Guo, L. Chen, H. Zuo, P. Zhao, and Q. Xia, "*In situ* green synthesis and characterization of sericin-silver nanoparticle composite with effective anti-bacterial activity and good biocompatibility," *Materials Science and Engineering: C,* vol. 80, pp. 509–516, 2017.

[30] B. D. Hall, D. Zanchet, and D. Ugarte, "Estimating nanoparticle size from diffraction measurements," *Journal of Applied Crystallography,* vol. 33, pp. 1335–1341, 2000.

[31] CLSI, *Performance Standards for Antimicrobial Susceptibility Testing: 24th Informational Supplement*, CLSI document M100-S24. Wayne, PA, USA: Clinical and Laboratory Standards Institute, 2014.

[32] Y. Dasaradhudu, and M.A. Srinivasan, "Synthesis and characterization of silver nanoparticles using co-precipitation method," *Materials Today: Proceedings,* vol. 33, pp. 720–723, 2020.

[33] E. Mahmoudi, W. L. Ang, G. Panomsuwan, O. Jongprateep, A. Wahab, L. Y. Ng, Ng, and M. M. Ba-Abbad, "Influence of graphite feedstock on the characteristics of silver-decorated graphene oxide and antimicrobial property," *Journal of Metals, Materials and Minerals,* vol. 31, pp. 143–150, 2021.

[34] H. M. Tahir, F. Saleem, S. Ali, Q. U. Ain, A. Fazal, M. Summer, R. Mushtaq, M. T. Zahid, I. Liaqat, and G. Murtaza, "Synthesis of sericin-conjugated silver nanoparticles and their potential antimicrobial activity," *Journal of Basic Microbiology,* vol. 60, no. 5, pp. 458–467, 2020.

[35] S. Rasheed, A. Amin, A. Sarwar, H. Saleem, and A. Hassan, "Evaluation of antimicrobial effect of silver nanoparticle based whey emulsions and edible films for the extension of shelf life of fruits and vegetables," *Current Microbiology*, vol. 80, p. 158, 2023.

[36] S. Srisod, K. Motina, T. Inprasit, and P. Pisitsak, "A green and facile approach to durable antimicrobial coating of cotton with silver nanoparticles, whey protein, and natural tannin," *Progress in Organic Coatings,* vol. 120, pp. 123–131, 2018.

[37] M. A. El-Bendary, S. S. Afifi, M. E. Moharam, S. M. A. El-Ola, A. Salama, E. A. Omara, M. N. Shaheen, A. A. Hamed, and N. A. Gawdat, "Biosynthesis of silver nanoparticles using isolated *Bacillus subtilis*: characterization, antimicrobial activity,

cytotoxicity, and their performance as antimicrobial agent for textile materials," *Preparative Biochemistry & Biotechnology,* vol. 51, no. 1, pp. 54–68, 2021.

[38] M. N. Bahabadi, F. H. Delavar, M. Mirbakhsh, K. Niknam, and S. A. Johari, "Assessment of antibacterial activity of two different sizes of colloidal silver nanoparticle (cAgNPs) against *Vibrio harveyi* isolated from shrimp *Litopenaeus vannamei*," *Aquaculture International,* vol. 25, pp. 463–472, 2017.

[39] Y. Zhou, and R. Tang, "Facile and eco-friendly fabrication of AgNPs coated silk for antibacterial and antioxidant textiles using honeysuckle extract," *Journal of Photochemistry and Photobiology B: Biology,* vol. 178, pp. 463–471, 2018.

[40] C. Chitichotpanya, P. Khwanmuang, W. Yamprayoonswat, S. Porntheeraphat, A. Jongkaewwattana, and P. Chitichotpanya, "Potent environmental-friendly virucidal medical textiles against coronavirus to combat infections during the COVID-19 pandemic," *Journal of Industrial Textiles,* vol. 51, pp. 6996S–7013S, 2022.

[41] M. Kim, S.-C. Jee, S. K. Shinde, B. M. Mistry, R. G. Saratale, G. D. Saratale, G. S. Ghodake, D.-Y. Kim, J.-S. Sung, and A. A. Kadam, "Green-synthesis of anisotropic peptone-silver nanoparticles and its potential application as anti-bacterial agent," *Polymers,* vol. 11, no. 2, p. 271, 2019.

[42] M. Jariyaboon, P. Masrinoul, J. Komaikul, K. Muenkaew, S. Juntarapornchai, K. Ketsuwan, E. Rodpai, S. Ruangdachsuwan, S. Palabodeewat, and C. Chitichotpanya, "Optimization of Ag-TiO_2 nanocomposite at a low toxicity dose as a self-virucidal disinfectant against COVID-19," *Emergent Materials,* vol. 6, pp. 1259–1272, 2023.

[43] P. RathnaKumari, P. Kolanchinathan, D. Siva, B. Abirami, V. Masilamani, G. John, S. Achiraman, and A. Balasundaram, "Antibacterial efficacy of seagrass Cymodocea serrulata-engineered silver nanoparticles against prawn pathogen *Vibrio parahaemolyticus* and its combative effect on the marine shrimp *Penaeus monodon*," *Aquaculture,* vol. 493, pp. 158–164, 2018.

[44] E. Haque, and R. Kumarasamy, "Bioengineered silver nanoparticle from *Spirulina platensis* in attenuating biofilm mediated virulence in *Vibrio parahemolyticus*: An in vitro and in vivo Approach," *International Journal of Pharmaceutical Investigation,* vol. 10, pp. 486–491, 2020.

[45] M. F. Saad, M. M. Elsayed, M. Khder, A. S. Abdelaziz, and A. S. El-Demerdash, "Biocontrol of multidrug resistant pathogens isolated from fish farms using silver nanoparticles combined with hydrogen peroxide insight to its modulatory effect," *Scientific Reports,* vol. 14, p. 7971, 2024.

[46] K. Bhatt, A. Kongor, M. Atharb, and V. Jain, "New views on the ingenious applications of Ag nanoparticles as a sensor for antibiotic detection and as a potent antimicrobial agent," *Journal of Metals, Materials and Minerals,* vol. 31, pp. 1–9, 2021.

[47] S. Agnihotri, S. Mukherji, and S. Mukherji, "Size-controlled silver nanoparticles synthesized over the range 5–100 nm using the same protocol and their antibacterial efficacy," *RSC Advances,* vol. 4, pp. 3974–3983, 2014.

[48] A. Sharma, N. Kaur, A. Nanda, M. Kaur, R. Sharma, and H. S. Sohal, "Recent advances in synthesis and bio-applications of natural stabilizers for metal nanoparticles," *Journal of Metals, Materials and Minerals,* vol. 34, p. 2145, 2024.